**Article:**

Wang, J.-D., Jiang, J.-J., Duan, F.-J. et al. (3 more authors) (2020) A novel fast resonance frequency tracking method based on the admittance circle for ultrasonic transducers. IEEE Transactions on Industrial Electronics, 67 (8). pp. 6864-6873. ISSN 0278-0046

https://doi.org/10.1109/tie.2019.2938476

# A Novel Fast Resonance Frequency Tracking Method Based on the Admittance Circle for Ultrasonic Transducers

Jin-dong Wang[a], Jia-jia Jiang[a], *Member, IEEE*, Fa-jie Duan[a*], Fu-min Zhang[a], Wei liu[b], *Senior Member, IEEE*, Xing-hua Qu[a]

***Abstract*—For ultrasonic systems, the resonance frequency tracking (RFT) is the most critical step. The rapid development in advanced material processing and microelectronics package has increased the demand of high speed RFT. Therefore, this paper proposes a fast RFT (FRFT) method according to the characteristics of piezoelectric transducers' (PT) admittance circle. In the proposed method, the PT is driven at two different frequencies, and the PT's admittance is collected and calibrated. Then, the PT's mechanical resonance frequency is derived using the admittance information after calibration. The proposed method is not affected by the parallel capacitor and the matching circuit. Additionally, the optimal initial values of the involved parameters are determined in order to improve the accuracy of the proposed method. Furthermore, an improved method based on multiple tracking is also provided. Simulations and experiments demonstrate that using the proposed FRFT method, the ultrasonic system can track the resonance frequency in a short time with high accuracy.**

***Index Terms*—Piezoelectric transducer, Resonance frequency tracking (RFT), Transducers, Ultrasonic welding.**

## I. Introduction

PIEZOELECTRIC transducers (PT) are widely used as the actuators to generate ultrasound for various purposes [1-3], such as machining semiconductor materials [4], biological tissue cutting [5] and ultrasonic welding [6-8]. When driving a PT, it is important that the PT should be excited at its mechanical resonance frequency $f_s$, as the highest power conversion is achieved at this frequency [9]. However, $f_s$ significantly fluctuates during the actual operation with acoustic load and environmental conditions [9, 10]. The typical PTs usually have high electric quality factor. Thus, the vibration amplitude is sensitive even to a relatively small degree of driving frequency offset. Therefore, it is essential to automatically tuned the actuated frequency in real-time in order to maintain the stable output of ultrasonic systems. This process is generally called resonance frequency tracking (RFT). Moreover, the actual action process time for many ultrasonic systems is extremely short, less than one second. Taking the automatic ultrasonic plastic welding for example, an ultrasonic welding system is applied in the automatic assembly line whose machining speed is over 50 pieces per minute, and the interconnection time between welding joint and welded component is less than 0.3 s. The RFT process must be finished within this time. Therefore, the tracking speed is also crucial for RFT methods [7].

This work was supported in part by the Tianjin Natural Science Foundations of China (Grant No. 17JCQNJC01100), National Natural Science Foundations of China (Grant No. 61501319, 51775377), National key research and development plan (2017YFF0204800), Young Elite Scientists Sponsorship Program By Cast of China (Grant No. 2016QNRC001), the key technologies R & D program of Tianjin (18YFZCGX00920) and National Key R&D Program of China (Grant No. 2018YFF0212702).
J. Wang and J. Jiang contributed equally to this work.
[*]F. Duan is the corresponding author (fjduan@tju.edu.cn).
[a] J. Wang, J. Jiang, F. Duan, F. Zhang and X. Qu are with the State Key Lab of Precision Measuring Technology & Instruments, Tianjin 300072, China, (e-mail: tju_jdwang@163.com; jiajiajiang@tju.edu.cn; fjduan@tju.edu.cn; zhangfumin@tju.edu.cn; quxinghua@tju.edu.cn).
[b] W. Liu is with the Department of Electronic and Electrical Engineering, University of Sheffield, UK, (e-mail: w.liu@sheffield.ac.uk).

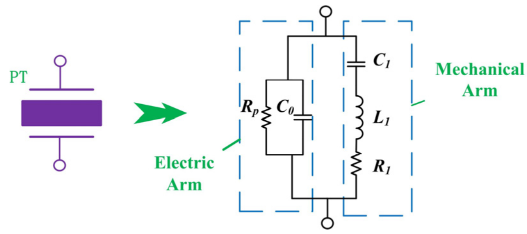


Fig. 1. Equivalent circuit model of an ultrasonic piezoelectric transducer.

Generally, a PT can be equivalent to a simple circuit shown consisting of two arms as shown in Fig. 1 [11, 12]. The first arm is the electric arm containing a parallel capacitor $C_0$ and a dielectric resistance $R_p$. While the other arm is the mechanic arm consisting of a dynamic capacitor $C_1$, a dynamic inductor $L_1$ and a dynamic resistance $R_1$. The mechanical resonance frequency $f_s$ can be calculated as

$$f_s = \frac{1}{2\pi\sqrt{L_1 C_1}}. \tag{1}$$

Over the last decades, RFT has become an important control issue and numerous RFT methods have been proposed in the literature. Most of these methods are based on phase-locked loop (PLL) technology that controls and tunes the driving frequency according to the phase difference between the current and the voltage applied to the PT. The PLL-based RFT methods [7, 10, 13-19] find and lock the zero-phase frequency $f_r$. However, $f_r$ is not equal to $f_s$ due to the presence of the parallel capacitance $C_0$ [17]. Although, $C_0$ can be compensated by matching networks with additional reactive components [7, 20, 21], the fluctuations of load, inductance and capacitance will cause the matching network invalid resulting in deviation of tracking results. Moreover, the PLL methods can also cause other serious problems, such as anti-resonance frequency tracking and loss of lock [14].

Furthermore, the above-mentioned PLL-based RFT methods usually involve a frequency search process [13, 22] that limits their tracking speed. In frequency search process, a dozen or more additional samples and calculations are required that consumes significant amount of time and is used for searching, not tracking. In [22], Zhang proposed a fast RFT method based on the binary search and fuzzy logical methods that can achieve a tracking time less than 2 ms and has good adaptability and flexibility. However, $f_r$ is regarded as the search target instead of $f_s$, and this fast RFT method still required 6-10 adjustments and could not avoid influence of $C_0$.

In order to avoid above-mentioned problems, several other RFT methods have been proposed in the literature that avoid tracking $f_s$ and rather track other characteristic frequency or value, such as tracking the parallel resonance frequency [13], the maximum power [5, 20, 23], the maximum admittance [24], or keep constant amplitude [16, 25-28]. These methods have achieved relatively good results. However, most of these methods involve complex structures and are only applicable to specific systems or fields. Besides, even if the output power is high enough, the working life of a PT not excited at the naturally resonant frequency ($f_s$) will be reduced.

In this paper, a fast RFT method is developed that can quickly capture the mechanical resonance frequency quickly, and can avoid the effects of $C_0$ and matching circuit. Firstly, the electrical characteristics of PTs are described and the drift of PT's admittance circle is demonstrated. Then, according to the features of the admittance circle, a fast resonance frequency tracking (FRFT) method is proposed where two points of the admittance circle are collected and calibrated to derive the center and the radius of the admittance circle, thereby the mechanical resonance frequency $f_s$ can be deduced. In the proposed method, only two samplings are involved in one tracking. Therefore, the implementation of ultra-fast frequency tracking is realized.

Moreover, in order to obtain high tracking accuracy, the values of several initial parameters involved in the proposed method are discussed and the optimum values are determined. Additionally, an improved method for high tracking accuracy is also proposed where multiple tracking is used. The addition of one or two extra tracking can significantly increase the tracking frequency. Lastly, experiments are conducted on an ultrasonic driving system to verify the feasibility of the proposed FRFT method.

## II. Principle of the Proposed FRFT Method

### A. Admittance Circle and Electric Characteristics of a PT

Based on the equivalent circuit shown in Fig. 1, a PT's admittance can be written as

$$Y = G + Bj = 1/R_p + j\omega C_0 + 1/[R_1 + j(\omega L_1 - 1/\omega C_1)]$$
$$= \{1/R_p + \omega^2 C_1^2 R_1/[(1-\omega^2 L_1 C_1)^2 + \omega^2 C_1^2 R_1^2]\}$$
$$+ j\{\omega C_0 + (1-\omega^2 L_1 C_1)\omega C_1/[(1-\omega^2 L_1 C_1)^2 + \omega^2 C_1^2 R_1^2]\}. \quad (2)$$

where $\omega$ is the angular frequency of the driving signal.

The conductance $G$ and susceptance $B$ are

$$G = \frac{1}{R_p} + \frac{\omega^2 C_1^2 R_1}{\left(1-\omega^2 L_1 C_1\right)^2 + \omega^2 C_1^2 R_1^2}, \quad (3)$$

$$B = \omega C_0 + \frac{\left(1-\omega^2 L_1 C_1\right)\omega C_1}{\left(1-\omega^2 L_1 C_1\right)^2 + \omega^2 C_1^2 R_1^2}. \quad (4)$$

From (2) and (3), following equation can be obtained:

$$\left(G - 1/R_p - 1/2R_1\right)^2 + \left(B - \omega C_0\right)^2 = \left(1/2R_1\right)^2. \quad (5)$$

Equation (5) shows that the locus of a PT's admittance near its resonant frequency can be sketched as a circle with radius $1/2R_1$ and center $(1/R_0 + 1/2R_1, \omega C_0)$ as shown in Fig. 2. Usually, $R_0$ is ignored due to its large value, thus the circle center can also be written as $(1/2R_1, \omega C_0)$. The value of $C_0$ is basically a fixed value once the PT's installation is done and can be easily measured at low frequencies before the operation. It can be seen from Fig. 2 that besides the mechanical resonance frequency $f_s$, there are also several other characteristic frequencies of a PT: the resonance frequency $f_r$, the anti-resonance frequency $f_a$, the parallel resonance frequency $f_p$, the maximum admittance frequency $f_m$ and the minimum admittance frequency $f_n$. Due to the existence of $C_0$, $f_s$ is not equal to $f_r$, and it is only possible to track $f_r$ using the PLL-based methods. In order to make $f_r$ and $f_s$ equal, reactive components including inductors and capacitors are applied to

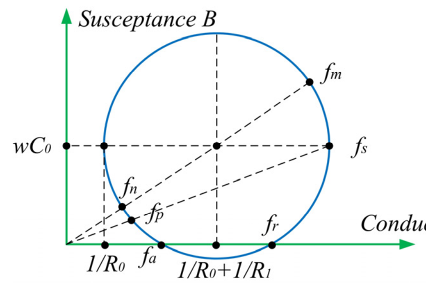

Fig. 2. Admittance circle of a PT and the characteristic frequencies.

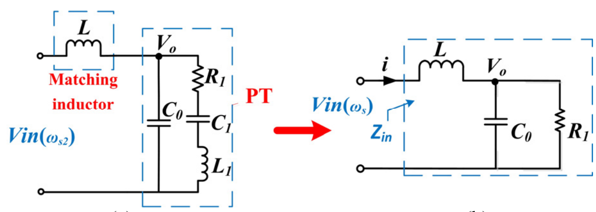

(a) (b)

Fig. 3. (a) Equivalent circuit model of a PT after matching by a inductor and (b) simplified circuit when mechanical resonance happens.

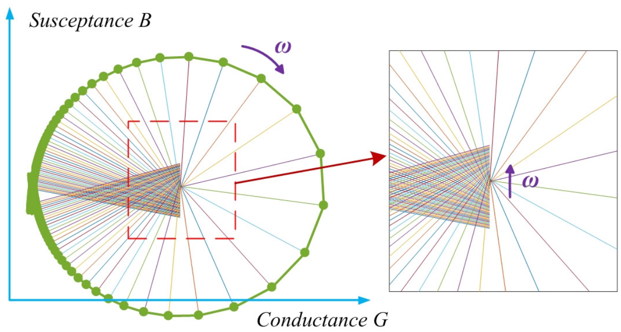


Fig. 4. Changing of the circle center of the admittance circle with $\omega$.

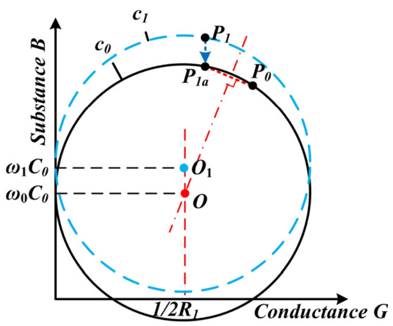


Fig. 5. The admittance circles of a PT under two different driving frequencies and the principle of the proposed FRFT method is also illustrated in this figure.

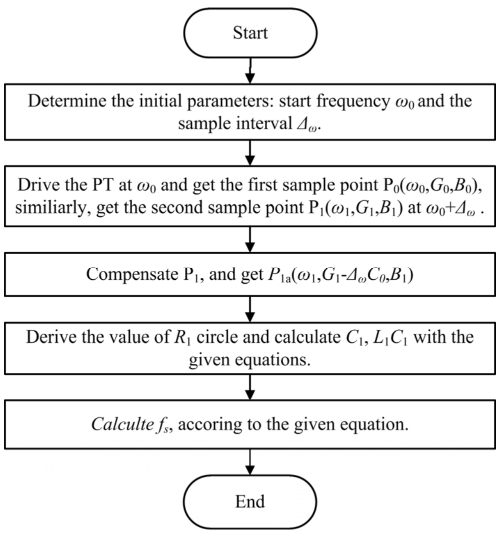


Fig. 6. Detail steps of the proposed FRFT method.

compensate PTs. Fig. 3 (a) shows an example where an inductor is applied to compensate the PT.

When the angular frequency of driving signal $\omega_{s2}$ is equal to $\omega_s$, which is the angular frequency of $f_s$, Fig. 3 (a) can be further simplified as Fig. 3 (b), and the complex impedance $Z_{in}$ can be expressed as:

$$Z_{in}(\omega_s) = j\omega_s L + \left(R_1 - j\omega_s R_1^2 C\right) / \left(1+\omega_s^2 R_1^2 C^2\right). \quad (6)$$

In order to make the immittance $Z_{in}(\omega_s)$ equal to zero, $L$ should satisfy the following equation:

$$L = R_1^2 C_0 / \left(1+\omega_s^2 R_1^2 C_0^2\right). \quad (7)$$

Equation (7) shows that the value of $L$ depends on $\omega_s$ and $R_1$ which shift over the operating conditions. Thus, in practice, the matching circuit may be invalid and can result in a considerable tracking error. This is the main problem of conventional PLL-based RFT methods.

### *B. The Proposed FRFT Method*

According to (5), the *G-B* points move in a circle, while the circle centers move along the vertical axis with the change of $\omega$, and their trajectories can be depicted as Fig. 4. The admittance circles are $(1/2R_1, \omega C_0)$ those whose abscissas are constant, while the ordinates are changing linearly with $\omega$. Each frequency corresponds to a *G-B* point in a different circle, such as the circles $c_0$ and $c_1$ illustrated in Fig. 5.

In the proposed method, according to the characteristics of PT's admittance circle, two points from the admittance circle are sampled and compensated to derive the admittance circle's center. Specifically, the value of $R_1$ is derived first, then the values of $L_1$ and $C_1$ are derived and lastly $f_s$ is calculated using (1). The detail steps of the proposed FRFT method are illustrated in Fig. 6.

Firstly, two significant parameters are determined. The first parameter is the starting frequency $\omega_0$ (corresponding frequency $f_0$), while the second is the sampling interval $\Delta\omega$ (corresponding frequency $\Delta f$), which is the frequency space between the two samplings. Both parameters are closely associated to the RFT accuracy. Secondly, the PT is operated at $\omega_0$, and $\omega_1 = \omega_0 + \Delta\omega$, and two sampling points $P_0(G_0, B_0)$ and $P_1(G_1, B_1)$ are obtained, which are on circles $c_0$ and $c_1$, respectively, as shown in Fig. 5.

In order to make $P_1$ and $P_0$ on the same circle, their ordinates need be compensated. As shown in Fig. 5, $P_1$ is adjusted to $P_{1a}(G_1, B_1 - \Delta\omega C_0)$. Both $P_{1a}$ and $P_0$ are now on the same circle $c_0$. The equation of the mid-perpendicular of the straight line $P_{1a}P_0$ is

$$B = -\frac{G_1 - G_0}{B_1 - \Delta\omega C_0 - B_0}\left(G - \frac{G_1+G_0}{2}\right) + \frac{B_1 - \Delta\omega C_0 + B_0}{2}. \quad (8)$$

Plugging the ordinate $\omega_0 C_0$ of $O$ into (8), the abscissa of $O$ can be obtained as

$$\frac{1}{2R_1} = -\frac{\left(\omega_0 C_0 - \frac{B_1 - \Delta\omega C_0 + B_0}{2}\right)\left(B_1 - \Delta\omega C_0 - B_0\right)}{G_1 - G_0} + \frac{G_1+G_0}{2}. \quad (9)$$

Then, $R_1$ can be calculated as:

$$R_1 = 1 \Big/ \left[G_1 + G_0 - \frac{\left(2\omega_0 C_0 - B_1 - \Delta\omega C_0 + B_0\right)\left(B_1 - \Delta\omega C_0 - B_0\right)}{G_1 - G_0}\right]. \quad (10)$$

Further, ignoring $R_0$, according to (3) and (4):

$$\frac{G}{B\text{-}\omega C_0} = \frac{\omega^2 C_1^2 R_1}{\left(1-\omega^2 L_1 C_1\right)\omega C_1} = \frac{R_1}{1/\omega C_1 - \omega L_1}, \quad (11)$$

$$1/\omega C_1 - \omega L_1 = \frac{R_1\left(B\text{-}\omega C_0\right)}{G}. \quad (12)$$

Equation (12) is the relationship of $C_1$ and $R_1$, and substituting the two sampling points $P_0$ and $P_1$ will provide the following:

$$\begin{cases} 1/\omega_0 C_1 - \omega_0 L_1 = \dfrac{R_1\left(B_0\text{-}\omega_0 C_0\right)}{G_0} \\ 1/\omega_1 C_1 - \omega_1 L_1 = \dfrac{R_1\left(B_1\text{-}\omega_1 C_0\right)}{G_1} \end{cases}. \tag{13}$$

From (13), $C_1$ can be solved as

$$C_1 = \frac{\omega_0 R_1\left(B_1\text{-}\omega_1 C_0\right)/G_1 - \omega_1 R_1\left(B_0\text{-}\omega_0 C_0\right)/G_0}{\omega_1/\omega_0 - \omega_0/\omega_1}. \tag{14}$$

Further, $L_1 C_1$ can be solved as

$$L_1 C_1 = \frac{1 - \omega_0 \cdot \dfrac{R_1\left(B_0\text{-}\omega_0 C_0\right)}{G_0} \cdot \dfrac{\dfrac{\omega_0 R_1\left(B_1\text{-}\omega_1 C_0\right)}{G_1} - \dfrac{\omega_1 R_1\left(B_0\text{-}\omega_0 C_0\right)}{G_0}}{\omega_1/\omega_0 - \omega_0/\omega_1}}{\omega_0^{\,2}}. \tag{15}$$

Finally, according to (1) and (15), $f_s$ can be derived as

$$f_s = \frac{\omega_0}{2\pi\sqrt{1 - \omega_0 \dfrac{R_1\left(B_0\text{-}\omega_0 C_0\right)}{G_0} \dfrac{\dfrac{\omega_0 R_1\left(B_1\text{-}\omega_1 C_0\right)}{G_1} - \dfrac{\omega_1 R_1\left(B_0\text{-}\omega_0 C_0\right)}{G_0}}{\omega_1/\omega_0 - \omega_0/\omega_1}}}. \tag{16}$$

Using (10) and (16), $f_s$ can be accurately calculated. In the above steps, only two samplings are taken to track the mechanical resonance frequency. Since no matching circuit is required in the proposed method, thereby the influence of matching failure and $C_0$ is avoided.

## III. Determining the Initial Parameters and An Improved Method

### A. Determination of the Initial Parameters

The initial parameters $\omega_0$ and $\Delta\omega$ of the proposed FRFT method are closely related to the tracking accuracy. Therefore, both parameters should be carefully determined. Specifically, it is an optimization problem that is determining the circle center with two points on the circle, when the circle center's vertical coordinates are known. As shown in Fig. 7, $f_{s0}$ is the experienced value of $f_s$, while $\Delta f_1$ is the difference between $f_{s0}$ and $f_0$. It can be seen from Fig. 7 that the frequency distribution in the admittance circle is not uniform, and there are several parameters involved in PT model. Multiple parameters make it difficult to determine the optimums of the initial parameters. Therefore, the trial and error method is selected to solve the problem.

In order to determine the optimums of $\Delta f_1$ and $\Delta f$, the tracking process of the FRFT method was simulated under different initial parameters and signal-to-noise ratio (SNR). The simulation was performed using *MATLAB 2016b* on a virtual PT whose parameters were set as $R_1$=178.96 Ω, $C_0$=4.491 nF, $L_1$=56.54 mH, $C_1$=0.2761 nF, hence $f_s$=40083 Hz (obtained from a real PT). The built-in additive white Gaussian noise (AWGN) function in the *MATLAB* was used to add Gaussian white noise to the simulated signals.

Then the steps shown in Fig. 6 were followed. Assuming $f_{s0}$ is equal to $f_s$, the frequency tracking results under different values $f_0$ and $\Delta f$ were derived and the results are shown in Fig. 8, where the RFT error is the difference between the tracked frequencies $f_{s1}$ and $f_s$, i.e. $error = f_{s1} - f_s$. The SNR were set as 40 dB and 50dB in Fig. 8 (a) and (b) respectively. Since the

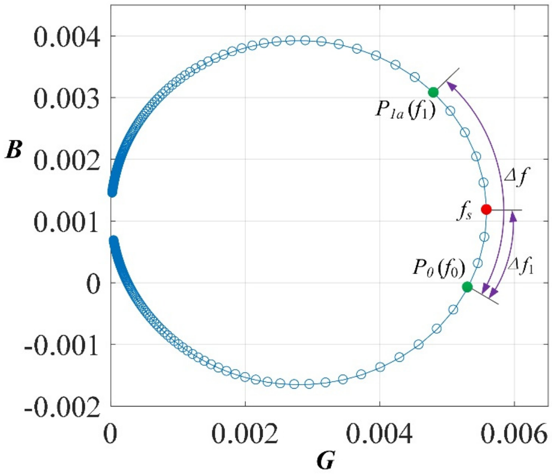


Fig. 7. Definition of initial parameters of the FRFT merthod.

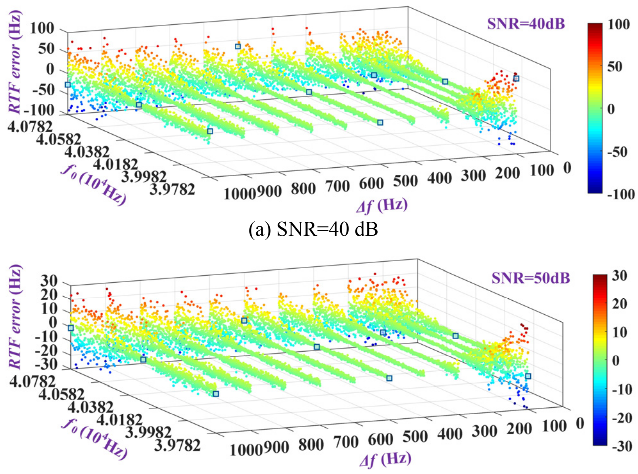


(a) SNR=40 dB

(b) SNR=50 dB

Fig. 8. Simulation results: RFT error under different $f_0$ and $\Delta f$, with different level white Gaussian noise is added to the simulating signal using AWGN function. It can be seen that when $\Delta f$ is set to about 300-400 Hz, the RFT error is the smallest.

sampling points are very dense (interval=1 Hz), the error levels can be represented exactly by the curves shown in Fig. 8. It can be seen from Fig. 8 that the influence of $\Delta f$ on the error is small and when $\Delta f$ is set to about 300 - 400 Hz, the RFT error is relatively smaller.

Next, the optimum of $f_0$ is determined. Similarly, setting $\Delta f$ to 300 Hz and 400 Hz, and SNR to 40 dB and 50 dB, the error- $\Delta f_1$ curves and their envelops (obtained by Hilbert transformation) are shown in Fig. 9. The curves in Fig. 9 have similar behaviors and the laws can be summarized as follows:

1) The error curves are symmetrical about the symcenter $\Delta f_{1sym}$ which is equal to $-\Delta f/2$, while $f_0$ is equal to $f_s - \Delta f/2$ at this point. When $\Delta f$ is 300 Hz, $\Delta f_{1sym}$ is -150 Hz, as shown in Fig. 9 (a) and (c). Similarly, when $\Delta f$ is 400 Hz, $\Delta f_{1sym}$ is -200 Hz, as shown in Fig. 9 (b) and (d).
2) When $f_s$ is between the two samplings, i. e. $f_0 < f_s < f_0 + \Delta f$, the RFT errors are small and the values are close. In contrast, when $f_s$ is outside the two samplings, the RFT

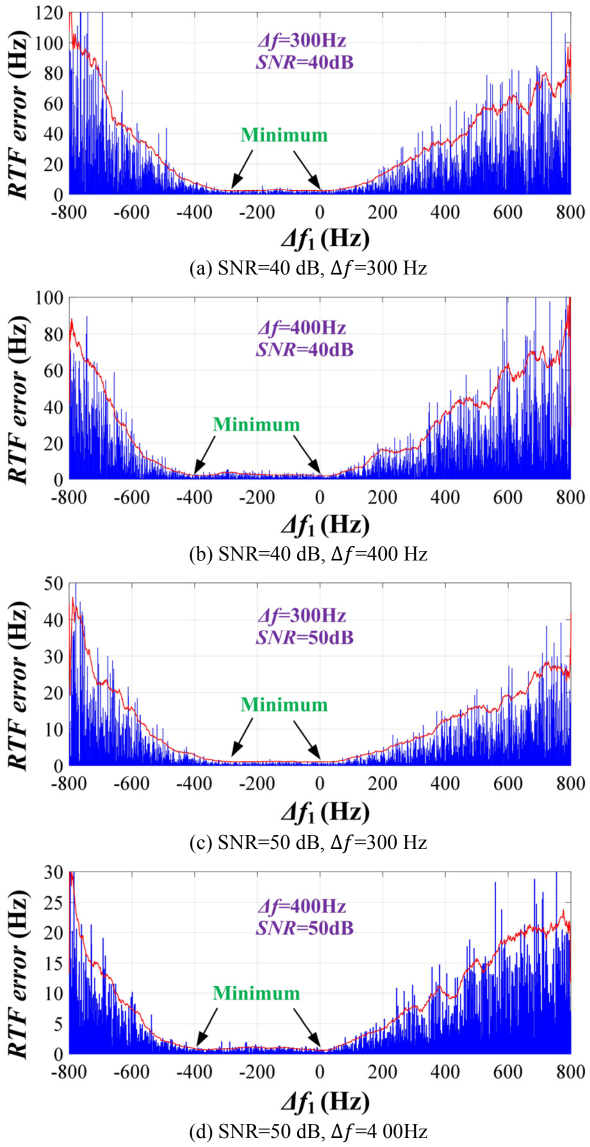


(a) SNR=40 dB, $\Delta f$=300 Hz

(b) SNR=40 dB, $\Delta f$=400 Hz

(c) SNR=50 dB, $\Delta f$=300 Hz

(d) SNR=50 dB, $\Delta f$=4 00Hz

Fig. 9. Simulation results: RFT error curves when $\Delta f$= 400 Hz and 300 Hz, SNR=50 dB and 40 dB, where the envelop is obtained by Hilbert transformation, and the minimum points is indicated by arrows. It can be seen that the curve distribution has obvious regularity.

error will increase rapidly.

3) There are two minimum values in the error curves. Each minimum error value corresponds to the case where $f_s$ is one of the two sampling points.

According to the above-mentioned laws, to ensure that $f_s$ falls into the range $[f_0,\ f_0+\Delta f]$, $f_0$ is determined as $f_{s0}-\Delta f/2$, where $f_{s0}$ is the reference value of $f_s$, and $\Delta f$ is determined as 400 Hz.

In conclusion, it is possible to obtain an optimal solution through the trial and error method. However, a general solution of this issue is not obtained, but the authors have found some rules about it. Further research is required to obtain a general optimal solution for different transducers.

## B. An Improved Method based on Multiple Tracking

The real-time $f_s$ is constantly changing, so it is difficult to determine $f_{s0}$ and often there is considerably large difference between $f_{s0}$ and $f_s$. According to the law-2 concluded in above sub-section, the difference between $f_{s0}$ and $f_s$ will induce a large tracking error. Therefore, a method based on multiple tracking is also proposed to improve the tracking accuracy.

The exact approach is to track more than one time. In the first tracking, $f_{01}$ is determined as $f_{s0}-\Delta f/2$, and in the second and third tracking, $f_{02}$ and $f_{03}$ are determined as $f_{s1}$ and $f_{s2}$,

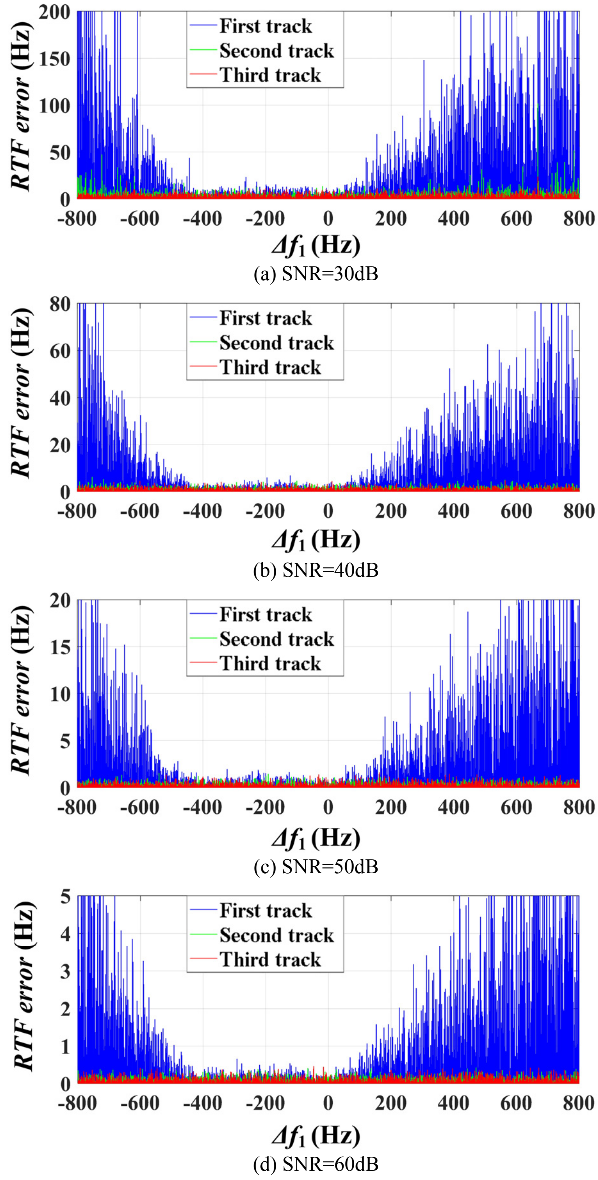


(a) SNR=30dB

(b) SNR=40dB

(c) SNR=50dB

(d) SNR=60dB

Fig. 10. RFT error - $\Delta f$ curves under different SNR, using the improved FRFT method where multiple tracking is used, i. e. the tracked frequency is used as the next initial frequency. It can be seen that the tracking accuracy is heavily improved after the second and the third tracking.

TABLE I
THE BIGGEST ERROR OF MULTIPLE TRACKING

| SNR | First track (Hz) | Second track (HZ) | Third track (HZ) |
|---|---|---|---|
| 30dB | 200 | 50 | 20 |
| *40dB* | 80 | 8 | 6 |
| *50dB* | 20 | 2 | 2 |
| *60dB* | 6 | 0.5 | 0.6 |

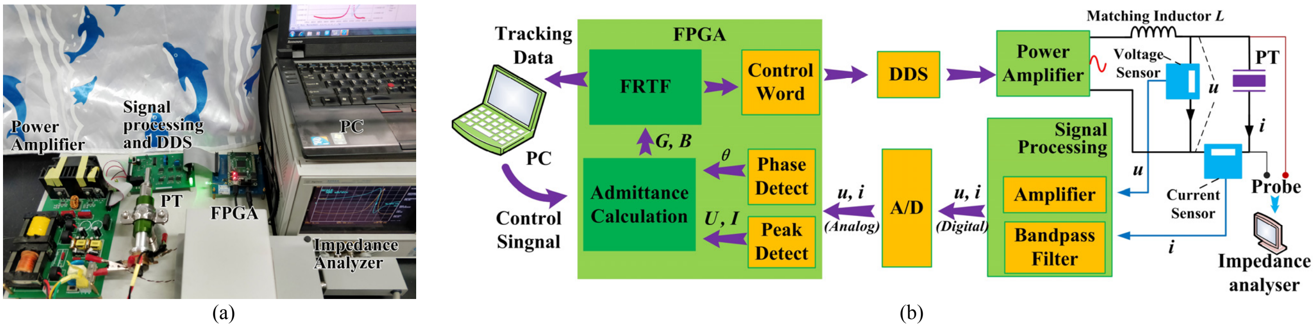


Fig.11. (a) The experimental setup and (b) the system's schematic diagram of the ultrasonic driving and control system using in the verification experiments.

respectively. As described in law-3, when the tracked frequency $f_{s1}$ is closer to $f_s$ than the initial frequency $f_0$, using the tracked frequency as the next initial frequency could improve the RFT accuracy. Thus, multiple tracking can increase tracking accuracy.

In order to test the multiple tracking based improved method, simulations under different values of SNR (30 dB, 40 dB, 50 dB and 60 dB) were performed on the same virtual PT mentioned in Part III-A where $\Delta f$ was set as 400Hz, and the results are shown in Fig. 10 and Table I.

It can be seen that after second or third tracking, the RFT accuracy is improved ten or more times in every situation. Moreover, in high noise level (SNR=30 dB), the third tracking improves the accuracy further. While in low noise level (SNR>40 dB), both the third and the second tracking provide similar accuracy.

## IV. Experiments and Discussion

### A. Experimental Setup

In order to verify the proposed FRFT method and the improved multiple tracking method, an ultrasonic driving system was designed and constructed. The experimental setup and its schematic diagram are illustrated in Fig. 11. A field-programmable gate array (FPGA) microchip *Altera Cyclone IV EP4CE10F17* (CLK rate 168 MHz) was used to calculate the admittance, realize the FRFT method and control the direct digital synthesis (DDS) chip *AD9850*. The driving signal generated by the DDS was amplified using the power amplifier (a self-developed class D switching power amplifier) to drive the PT after inductance matching. The hall voltage and the current sensors were used to sample the voltage $u$ across the PT and the current $i$ flowing through the PT, respectively. The sampled signals were amplified and filtered by the signal processing circuit (SPC), and then were synchronously converted to digital signals using the analog-to-digital (A/D) *AD9826* circuit. The amplitudes $U$, and $I$ of $u$ and $i$, respectively, and their phase difference $\theta$ were detected by the FPGA. The conductance $G$ and the susceptance $B$ can be calculated as:

$$G = I\cos\theta / U, \tag{17}$$

$$B = I\sin\theta / U. \tag{18}$$

Furthermore, the real-time tracking data including the initial frequency and the tracked frequencies were transferred to the top computer (PC).

The experimental system can also implement other PLL-based tracking methods. The basic diagram of PLL is shown in Fig. 12 (a). Nowadays, the microprocessor based digital PLL are common. In this condition, the lock-time more depends on the convergence speed and the complexity of the tracking algorithm, and the pull-in time can better represent the speed of the system than the bandwidth. Fig. 12 (b) shows the diagram of traditional PLL-based RFT methods. The pull-in time $T_{p1}$ can be expressed as the product of the number of cycles $N_1$ and the computation time $T_1$ of each circle, that is:

$$T_{p1} \approx N_1 \cdot T_1, \tag{19}$$

where $T_1$ is the sum of $t_1$, $t_2$ and $t_3$, which are the time delay of SPC, the time of admittance calculation, and the time of phase comparison, respectively. Assuming that the search range is 2000Hz, and the tolerance is 5Hz. The binary search is one of the fastest search algorithms. Thus, using binary search algorithm, $N_1$ can be estimated as:

$$N_1 > 1 + \log_2 \frac{2000}{5} \approx 10. \tag{20}$$

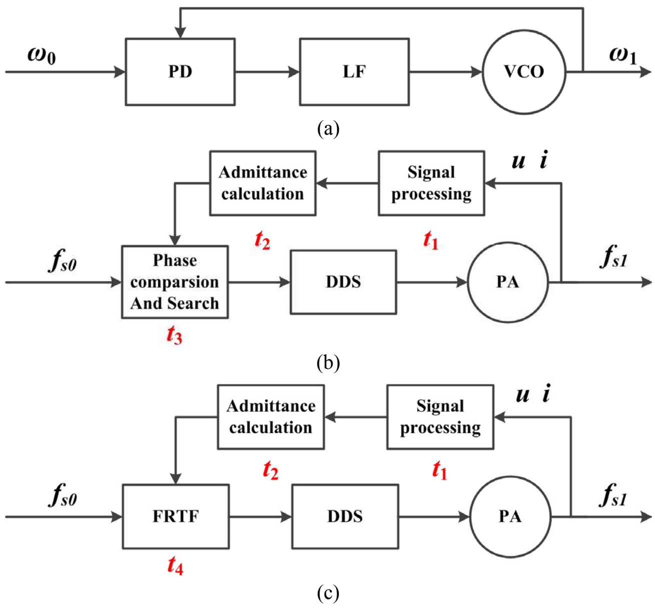


Fig. 12. (a) Basic diagram of PLL, (b) the diagram of traditional PLL based RFT methods and (c) the diagram of the proposed FRFT methods, where PD is the phase detector, LF is the loop filter and VCO is the voltage-controlled oscillator.

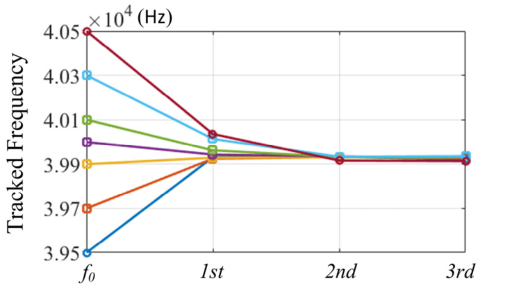


(a) Experimental results in high power conditions (400 W)

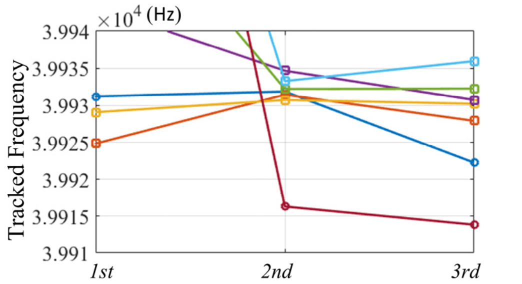


(b) Local magnification of (a)

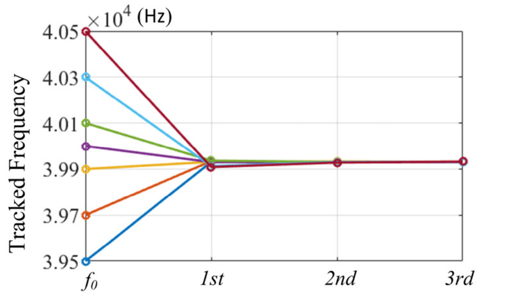


(c) Experimental results in low power conditions (100 W)

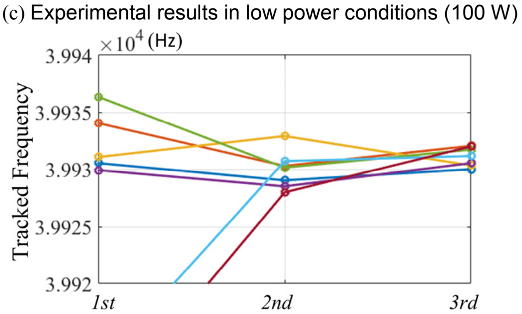


(d) Local magnification of (c)

Fig. 13. Experimental results that using the proposed FRFT method: (a) at high power conditions (400 W) and (c) at low power conditions (100 W), and (c), (d) are the local magnification of (a), (c) respectively. The x-coordinate is the tracking ordinal.

Fig. 12 (c) shows the diagram of the proposed FRFT method. The main difference in Fig. 12 (b) and (c) is that the process of phase comparison and search is replaced by the proposed FRFT method. Similarly, the pull-in time $T_{p2}$ can be expressed as:

$$T_{p2} \approx N_2 \cdot T_2, \tag{21}$$

where $T_2$ is the sum of $t_1$, $t_2$ and $t_4$, and $t_4$ is the calculation time of the proposed FRFT method. The number of cycles $N_2$ is 2 or 4. Since the experimental conditions and the calculating processes are nearly the same, both $T_1$ and $T_2$ are also approximately the same. Therefore, the number of circles can represent the tracking speed well. Since, $N_2$ is significantly less than $N_1$, thus the speed of the proposed FRFT method is significantly faster than the conventional PLL-based methods.

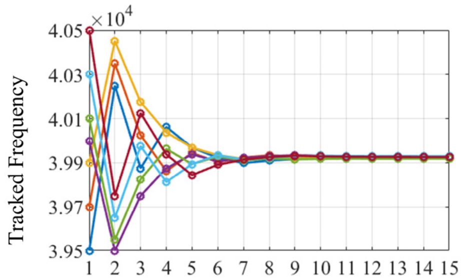


(a) Experimental results in high power conditions (400 W)

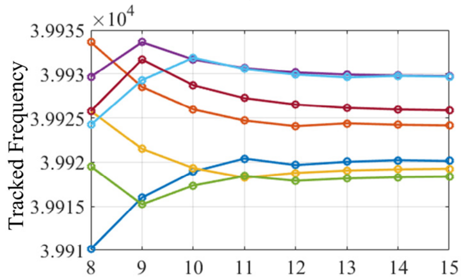


(b) Local magnification of (a)

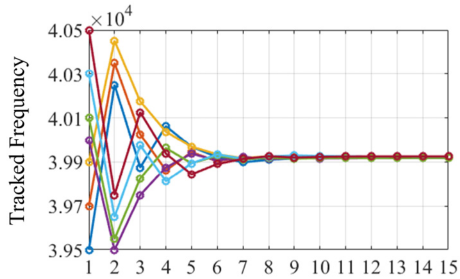


(c) Experimental results in low power conditions (100 W)

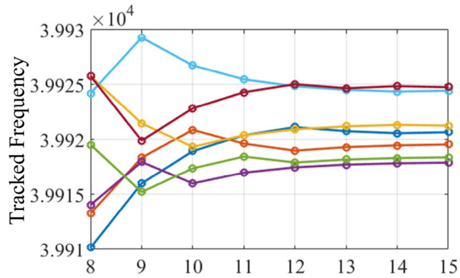


(d) Local magnification of (c)

Fig. 14. Experimental results that using the traditional PLL based method with a binary search algorithm: (a) at high power conditions (400 W) and (c) at low power conditions (100 W), and (c), (d) are the local magnification of (a), (c) respectively. The x-coordinate is the adjustment ordinal.

## *B. Experimental Results*

Under the laboratory environment, the PT's mechanical resonance frequency measured by an impedance analyzer *Agilent4294A* was 39930 Hz. The experiments were conducted on both high power (400 W) and low power (100 W) conditions, and $f_0$ was set to different values around the reference frequency (40 kHz). In general, the SNR decreased with the increase in the power.

Fig. 13 shows the results obtained using the proposed FRFT method and the multiple tracking method. The second tracking is taken as the results. Fig. 14 shows the results obtained using

TABLE II
TIME CONSUMPTION OF TWO METHODS

| Method | $t_1$ (ms) | $t_2$ (ms) | $t_3$ (ms) | $t_4$ (ms) | $N$ | $T_p$ (ms) |
|---|---|---|---|---|---|---|
| FRFT | <0.1 | 0.2 | 0 | 0.1 | 4 | 1.5 |
| *Binary search* | <0.1 | 0.2 | <0.1 | 0 | 12 | 4.0 |

the traditional PLL-based method with a binary search algorithm. The pull-in times of both approaches are listed in Table II. $T_{p1}$ is slightly smaller than $T_{p2}$, while $N_1$ is much larger than $N_2$. It can be seen from Figs. 13 and 14 that both the PLL-based and the proposed FRFT methods have approximately the same accuracies (about 15 Hz, see Figs. 13 (b) and 14 (b)) in high power conditions. However, in low power conditions, the FRFT method (within 5 Hz) provides much better accuracy than the traditional PLL-based method (see Figs. 13 (d) and 14 (d)). Moreover, the pull-in time (1.5 ms) of the FRFT method is much less than that of the conventional PLL-based method (4 ms). The traditional method requires at least 12 adjustments while only four adjustments (two tracking) are required in the proposed FRFT method.

### *C. Discussion*

In conclusion, the experimental results demonstrate that the ultrasonic system using the proposed FRFT method has better accuracy performance and faster tracking speed than using the traditional PLL-based method especially in lower power conditions (high SNR).

It is worth mentioning here that in the process of solving $f_s$, some computation is involved, which requires certain hardware resources such as medium or high-performance FPGA. If this condition is not met, the tracking speed may slow down. Besides, other control issues such as impedance matching, constant power control and constant amplitude are also very important for ultrasonic systems. Combining these methods makes high performance ultrasonic system possible.

## V. CONCLUSION

The paper proposes a novel fast resonance frequency tracking method for ultrasonic transducers. The proposed method requires only two adjustments of driving frequency to track the mechanical resonance frequency. Moreover, the mechanical resonance frequency is directly solved according to the collected data rather than using the search algorithms. The proposed FRFT method can effectively avoid the influence of $C_0$ and matching circuit and has faster tracking speed than the traditional PLL-based methods. Additionally, an improved method based on multiple tracking of the proposed FRFT method is also proposed, where two or four extra adjustments are needed but the tracking accuracy can be increased significantly. In order to validate the proposed method, experiments were conducted on an ultrasonic driving and control system. The obtained results demonstrate that, using the improved FRFT method can achieve higher tracking accuracy and faster tracking speed than the traditional methods.

Moreover, the proposed FRFT method behaves much better in high SNR conditions. Consequently, considering both of these issues, the proposed FRFT method is more suitable for high performance systems. Nowadays, the development of instruments is moving towards high performance, small scale and high precision, thus the proposed FRFT method has high application value and development potential.

Additionally, there is still room for improvement for the FRFT method. Further research work is required to provide a general initial parameter setting method for different types of PTs.

## REFERENCES


[1] G. Harvey, A. Gachagan, and T. Mutasa, "Review of high-power ultrasound-industrial applications and measurement methods," *IEEE Transactions on Ultrasonics Ferroelectrics & Frequency Control,* vol. 61, no. 3, pp. 481-95, 2014.

[2] T. J. Mason, "Ultrasonic cleaning: An historical perspective," *Ultrasonics Sonochemistry,* vol. 29, pp. 519-523, 2016.

[3] K. Ding, Y. Fu, H. Su, H. Xu, F. Cui, and Q. Li, "Experimental studies on matching performance of grinding and vibration parameters in ultrasonic assisted grinding of SiC ceramics," *International Journal of Advanced Manufacturing Technology,* vol. 88, no. 9-12, pp. 2527-2535, 2017.

[4] B. T., ASPINWALL, K. D., WISE, and L. H. M., "Review on ultrasonic machining," *Int.j.mach.tools Manuf,* vol. 38, no. 4, pp. 239-255, 1998.

[5] X. Liu, A. I. Colli-Menchi, J. Gilbert, D. A. Friedrichs, K. Malang, and E. Sánchez-Sinencio, "An Automatic Resonance Tracking Scheme With Maximum Power Transfer for Piezoelectric Transducers," *IEEE Transactions on Industrial Electronics,* vol. 62, no. 11, pp. 7136-7145, 2015.

[6] F. Wang, H. Zhang, C. Liang, Y. Tian, X. Zhao, and D. Zhang, "Design of High-Frequency Ultrasonic Transducers With Flexure Decoupling Flanges for Thermosonic Bonding," *IEEE Transactions on Industrial Electronics,* vol. 63, no. 4, pp. 2304-2312, 2016.

[7] Y. Tao, L. Hwachun, L. Dongheon, S. Song, K. Dongok, and P. Sungjun, "Design of LC Resonant Inverter for Ultrasonic Metal Welding system," in International Conference on Smart Manufacturing Application, 2016.

[8] Y. He, Y. Hu, X. Chen, J. Gao, Z. Yang, K. Zhang, Y. Chen, Y. Zhang, H. Tang, and Y. Ao, "Ultrasonic power closed-loop control on wire bonder," in Electronics Packaging Technology Conference, 2017, pp. 691-695.

[9] A. Arnau, T. Sogorb, and Y. Jiménez, "A new method for continuous monitoring of series resonance frequency and simple determination of motional impedance parameters for loaded quartz-crystal resonators," *IEEE Transactions on Ultrasonics Ferroelectrics & Frequency Control,* vol. 48, no. 2, pp. 617-23, 2001.

[10] C. H. Lin, Y. Lu, H. J. Chiu, and C. L. Ou, "Eliminating the Temperature Effect of Piezoelectric Transformer in Backlight Electronic Ballast by Applying the Digital Phase-Locked-Loop Technique," *IEEE Transactions on Industrial Electronics,* vol. 54, no. 2, pp. 1024-1031, 2007.

[11] S. Sherrit, H. D. Wiederick, B. K. Mukherjee, and M. Sayer, "An accurate equivalent circuit for the unloaded piezoelectric vibrator in the thickness mode," *Journal of Physics D Applied Physics,* vol. 30, no. 16, pp. 2354, 1997.

[12] X. Li, P. Harkness, K. Worrall, R. Timoney, and M. Lucas, "A parametric study for the design of an optimized ultrasonic-percussive planetary drill tool," *IEEE Trans Ultrason Ferroelectr Freq Control,* vol. 99, pp. 1-1, 2017.

[13] L. C. Cheng, Y. C. Kang, and C. L. Chen, "A Resonance-Frequency-Tracing Method for a Current-Fed Piezoelectric Transducer," *IEEE Transactions on Industrial Electronics,* vol. 61, no. 11, pp. 6031-6040, 2014.

[14] H. J. Dong, J. Wu, G. Y. Zhang, and H. F. Wu, "An improved phase-locked loop method for automatic resonance frequency tracing based on static capacitance broadband compensation for a high-power ultrasonic transducer," *IEEE Transactions on Ultrasonics Ferroelectrics & Frequency Control,* vol. 59, no. 2, pp. 205-10, 2012.

[15] Y. Kuang, M. R. Sadiq, S. Cochran, and Z. Huang, "Ultrasonic cutting with resonance tracking and vibration stabilization," in Ultrasonics Symposium, 2013, pp. 843-846.

[16] W. Shi, H. Zhao, J. Ma, and Y. Yao, "An Optimum-Frequency Tracking Scheme for Ultrasonic Motor," *Ultrasonics,* vol. 90, no. 6, pp. 63, 2018.
[17] Y. Kuang, Y. Jin, S. Cochran, and Z. Huang, "Resonance tracking and vibration stablilization for high power ultrasonic transducers," *Ultrasonics,* vol. 54, no. 1, pp. 187-194, 2014.
[18] H. Li, and Z. Jiang, "On Automatic Resonant Frequency Tracking in LLC Series Resonant Converter Based on Zero-Current Duration Time of Secondary Diode," *IEEE Transactions on Power Electronics,* vol. 31, no. 7, pp. 1-1, 2015.
[19] W. Feng, P. Mattavelli, and F. C. Lee, "Pulsewidth Locked Loop (PWLL) for Automatic Resonant Frequency Tracking in LLC DC–DC Transformer (LLC -DCX)," *IEEE Transactions on Power Electronics,* vol. 28, no. 4, pp. 1862-1869, 2013.
[20] X. Jiang, X. Zhu, C. Y. Y. Wong, D. Zhang, and D. Geng, "Theory of Series Inductance Matching to Transducer at Pre-Mechanical Resonance Zone in Ultrasonic Vibration Cutting," *IEEE Transactions on Industrial Electronics,* vol. PP, no. 99, pp. 1-1.
[21] Y. Yang, X. Wei, L. Zhang, and W. Yao, "The Effect of Electrical Impedance Matching on the Electromechanical Characteristics of Sandwiched Piezoelectric Ultrasonic Transducers," *Sensors,* vol. 17, no. 12, pp. 2832, 2017.
[22] H. Zhang, F. Wang, D. Zhang, L. Wang, Y. Hou, and X. Tao, "A new automatic resonance frequency tracking method for piezoelectric ultrasonic transducers used in thermosonic wire bonding," *Sensors & Actuators A Physical,* vol. 235, pp. 140-150, 2015.
[23] S. Ben-Yaakov, and S. Lineykin, "Maximum power tracking of piezoelectric transformer HV converters under load variations," *IEEE Transactions on Power Electronics,* vol. 21, no. 1, pp. 73-78, 2006.
[24] B. Mortimer, T. D. Bruyn, J. Davies, and J. Tapson, "High power resonant tracking amplifier using admittance locking," *Ultrasonics,* vol. 39, no. 4, pp. 257-261, 2001.
[25] X. Jiang, X. Zhang, X. Zhu, H. Sui, and D. Zhang, "Study of Phase Shift Control in High-speed Ultrasonic Vibration Cutting," *IEEE Transactions on Industrial Electronics,* vol. PP, no. 99, pp. 1-1, 2017.
[26] S. Ghenna, F. Giraud, C. Giraud-Audine, and M. Amberg, "Vector Control of Piezoelectric Transducers and Ultrasonic Actuators," *IEEE Transactions on Industrial Electronics,* vol. 65, no. 6, pp. 4880-4888, 2018.
[27] J. Wang, J. Jiang, F. Duan, S. Cheng, C. Peng, W. Liu, and X. Qu, "A High-Tolerance Matching Method against Load Fluctuation for Ultrasonic Transducers," *IEEE Transactions on Power Electronics*, pp. 1-1, 2019.
[28] Z. Long, Z. Pan, C. Li, and J. Zhang, "Constant amplitude control of high-power ultrasonic drive system," in IEEE International Conference on Information & Automation, 2014.

**Jin-dong Wang** was born in AnHui, China, in 1995. He received the B.S. degree in measuring and controlling technologies and instruments from Tianjin University (State Key Lab of Precision Measuring Technology & Instruments), Tianjin, China, in 2016, where he is currently working toward the Ph.D. degree at the school of precision instruments & opto-electronics engineering.

His research interests include high power ultrasound, actuating circuits of piezoelectric transducers and precision opto-electrical measurement.

**Jia-jia Jiang** was born in HuBei, China, in 1986. He received the B.S. degrees from HeBei Normal University and the M.S. degree and Ph.D. degree from Tianjin University (State Key Lab of Precision Measuring Technology & Instruments), Tianjin, China, in 2011 and 2014, respectively. He is currently an associate professor in Tianjin University (State Key Lab of Precision Measuring Technology & Instruments).

His research interest focuses on underwater acoustic detection, underwater acoustic communication, array signal processing.

**Fa-jie Duan** was born in HuNan, China, in 1968. He received the M.S. degrees from Tianjin University and the Ph.D. degree from Tianjin University (State Key Lab of Precision Measuring Technology & Instruments), Tianjin, China, in 1991 and 1994, respectively. He worked as a professor at Tianjin University (State Key Lab of Precision Measuring Technology & Instruments) since 2004.

His research interest focuses on the design of the array system, array signal processing, acoustic detection of marine. He was named the National New Century Excellent Talents of Ministry of Education in 2005. He is the author or coauthor of over 120 papers and holds seven patents.

**Fu-min Zhang** was born in NeiMengGu, China, in 1982. He received the B.E. degree in measuring and controlling technologies and instruments from Harbin Institute of Technology, China, in 2004 and the Ph.D. degree from Tianjin University, China (State Key Lab of Precision Measuring Technology & Instruments) in 2009. He is currently an associate professor in Tianjin University (State Key Lab of Precision Measuring Technology & Instruments).

His current research interests include precision opto-electrical measurement and absolute distance measurement.

**Wei Liu** received the B.Sc. and L.L.B. degrees from Peking University, China, in 1996 and 1997, respectively, the M.Phil. degree from The University of Hong Kong in 2001, and the Ph.D. degree from the School of Electronics and Computer Science, University of Southampton, U.K., in 2003. He held a post-doctoral position at the Imperial College London. Since 2005, he has been with the Department of Electronic and Electrical Engineering, University of Sheffield, U.K., as a Lecturer and then as a Senior Lecturer. He has authored over 230 journal and conference papers, three book chapters, and a research monograph about wideband beamforming (Wideband Beamforming: Concepts and Techniques, Wiley, 2010).

His research interests are in sensor array signal processing, blind signal processing, multivariate signal processing and their various applications in wireless communications, radar, sonar, satellite navigation, human computer interface, and renewable energy exploitation.

**Xing-hua Qu** was born in ShanDong province, China, in 1956. He received the B.S. degree, the M.S. degree and the Ph.D. degree from Tianjin University (State Key Lab of Precision Measuring Technology & Instruments), China, in 1982. 1988, and 2003, respectively. He worked as a professor at Tianjin University (State Key Lab of Precision Measuring Technology & Instruments) since 2004.

His research interests are in precision opto-electrical measurement and precision instrument design. He is the author or coauthor of over 199 papers.